actuators

MDPI

Article

Addressing EMI and EMF Challenges in EV Wireless Charging with the Alternating Voltage Phase Coil

Zeeshan Shafiq [1], Tong Li [1], Jinglin Xia [2], Siqi Li [3,*], Xi Yang [4,*] and Yu Zhao [4]

[1] Department of Transportation Engineering, Kunming University of Science and Technology, Kunming 650500, China; shafiq.xeeshan@gmail.com (Z.S.); litongkm410@stu.kust.edu.cn (T.L.)
[2] Facility of Mechanical and Electrical Engineering, Kunming University of Science and Technology, Kunming 650500, China; xiajl22@kust.edu.cn
[3] Department of Electrical Engineering, Kunming University of Science and Technology, Kunming 650500, China
[4] Yunnan Energy Research Institute Co., Ltd., Kunming 650500, China; zhaoy32933@cnyeig.com
* Correspondence: lisiqi@kust.edu.cn (S.L.); yangxi@cnyeig.com (X.Y.)

Abstract: Wireless charging technologies are widely used in electric vehicles (EVs) due to their advantages of convenience and safety. Conventional wireless charging systems often use planar circular or square spiral windings, which tend to produce strong electric fields (E-fields), leading to electromagnetic interference (EMI) and potential health risks. These standard coil configurations, while efficient in energy transfer, often fail to address the critical balance between E-field emission reduction and power transfer effectiveness. This study presents an "Alternating Voltage Phase Coil" (AVPC), an innovative coil design that can address these limitations. The AVPC retains the standard dimensions of traditional square coils (400 mm in length and width, with a 2.5 mm wire diameter and 22 turns), but introduces a novel current flow pattern called Sequential Inversion Winding (SIW). This configuration of the winding significantly reduces E-field emissions by altering the sequence of current through its loops. Rigorous simulations and experimental evaluations have demonstrated the AVPC's ability to lower E-field emissions by effectively up to 85% while maintaining charging power. Meeting stringent regulatory standards, this advancement in the proposed coil design method provides a way for WPT systems to meet stringent regulatory standards requirements while maintaining transmission capability.

Keywords: electric vehicles (EVs); electromagnetic field exposure; wireless power transfer; Alternating Voltage Phase Coil (AVPC); E-field mitigation in charging systems; coil designs

Citation: Shafiq, Z.; Li, T.; Xia, J.; Li, S.; Yang, X.; Zhao, Y. Addressing EMI and EMF Challenges in EV Wireless Charging with the Alternating Voltage Phase Coil. *Actuators* **2024**, *13*, 324. https://doi.org/10.3390/act13090324

Academic Editor: Dong Jiang

Received: 4 July 2024
Revised: 17 August 2024
Accepted: 23 August 2024
Published: 26 August 2024

1. Introduction

Wireless charging technology, characterized by its non-contact method of energy transfer, has revolutionized the convenience and safety of powering devices across various applications [1]. This technology facilitates the transfer of power without physical connections [2], finding use in diverse fields such as biomedical devices for remote healthcare monitoring [3], logistic optimization through unmanned warehousing [4], and advanced navigation systems for expansive marine exploration [5]. Originating over a century ago with basic inductive charging methods [6], wireless charging has progressively evolved into sophisticated forms like resonant inductive coupling and capacitive coupling [7,8], broadening its applicability. Despite these advancements, the technology faces significant challenges that hinder its wider adoption, particularly in high-power applications such as electric vehicles (EVs) [9]. These challenges include electromagnetic interference (EMI) and electromagnetic field (EMF) leakage, especially the electric field (E-field) component, which poses safety risks and reduces system efficiency [10,11]. Innovative solutions are needed to offer high performance and environmental compatibility [12], focusing on mitigating E-field emissions while maintaining efficient power transfer [13].

Previous research efforts in wireless charging coil design have focused on optimizing coil geometry [14], investigating novel materials, and developing advanced control strategies [15] to enhance coupling efficiency, reduce EMF leakage, and minimize EMI [16,17]. However, existing approaches, such as the distributed compensation topology [18], have limitations in coil design flexibility and overall system performance [19,20]. Most state-of-the-art wireless charging systems rely on passive shielding techniques [21], like metal plates near the coils or the implementation of alternative coil geometries, to mitigate EMF exposure risks [15,22]. While these methods effectively shield EMFs [23], they increase the charging units' size and complexity, introducing challenges such as enhanced parasitic capacitance [24], which can exacerbate conductive common mode noise issues and complicate compliance with stringent EMC standards [25,26].

In addition to shielding, optimized coil design, and active field cancelation techniques, the spread spectrum technique has emerged as another effective approach for reducing leakage fields and EMI in wireless charging systems. This technique, based on either random or periodic modulations, has been explored in recent studies [27]. The spread spectrum approach works by distributing the energy of the electromagnetic fields over a wider frequency range, thereby reducing the peak field strengths and minimizing potential interference with other electronic devices. While this technique has shown promise in mitigating leakage fields and EMI, it often requires more complex control systems and may introduce challenges in terms of power transfer efficiency and compatibility with existing wireless charging standards [28], as well as compliance with the ICNIRP guidelines and the European Directive limit for public human exposure to EMF at 85 kHz, set at 87 V/m [29]. Nonetheless, the spread spectrum technique represents a valuable addition to the arsenal of methods available for addressing the critical issues of electromagnetic compatibility and safety in wireless charging applications.

In response to these challenges, this paper introduces the Alternating Voltage Phase Coil (AVPC), a novel coil design optimized for EV wireless charging systems. The AVPC addresses key issues in traditional wireless charging systems by significantly reducing EMI and the E-field component of EMF leakage [22,30]. This study prioritizes the reduction in E-field emissions over leakage magnetic fields because E-fields are the primary contributor to potential health risks [31] and electromagnetic compatibility issues in wireless charging systems [32,33], in line with the ICNIRP guidelines and the European Directive limit for public human exposure to EMF [29]. By focusing on E-field mitigation, the AVPC aims to address the most pressing safety concerns while maintaining efficient power transfer through the intentional preservation of the H-field [24]. This unique approach to mitigating E-field emissions sets the AVPC apart from other state-of-the-art solutions. While existing techniques, such as the use of ferrite shields [23,34] or the implementation of metamaterials [35], have shown promise in reducing electromagnetic interference, they often come with trade-offs in terms of system complexity, cost, and power transfer efficiency [25]. In contrast, the AVPC's innovative design achieves significant E-field reduction through its unique coil geometry and current flow pattern, without compromising on power transfer efficiency or requiring additional complex components [15]. This sets the AVPC apart as a potentially game-changing solution for the wireless charging industry, offering a simpler, more efficient, and more effective approach to addressing the essential challenges of electromagnetic compatibility and safety in high-power wireless charging applications [26]. Its superiority lies in its innovative geometry, which minimizes electromagnetic emissions while maintaining high power transfer, similar to traditional coils [36]. Additionally, by its unique coil structure, the AVPC does not need the additional capacitors for maintaining a uniform magnetic field (H-field) distribution similar to traditional coil designs, as has been carried out in the distributed compensation topologies [37], which is essential for the reduction in E-field and optimal energy transmission. The AVPC's innovative Sequential Inversion Winding (SIW) technique creates an alternating high and low voltage arrangement across adjacent turns, ensuring effectively out-of-phase voltages that lead to opposing and canceling electric fields, significantly reducing overall E-field emissions. The development

of the AVPC offers practical advantages for wireless charging systems and contributes to the fundamental understanding of electromagnetic field behavior in these systems.

This study provides new insights into the relationship between coil geometry, current flow patterns, and the resulting electromagnetic field characteristics through the design and analysis of the AVPC. The architecture of EV wireless charging systems, as illustrated in Figure 1, involves several essential components, including grid frequency rectifiers, inverters, coupling coils, and network compensation, which must function cohesively to achieve efficient and safe power transmission. The coupling coil plays a central role in the wireless transfer of energy, and has been the focus of substantial research and development efforts aimed at enhancing its performance and safety features.

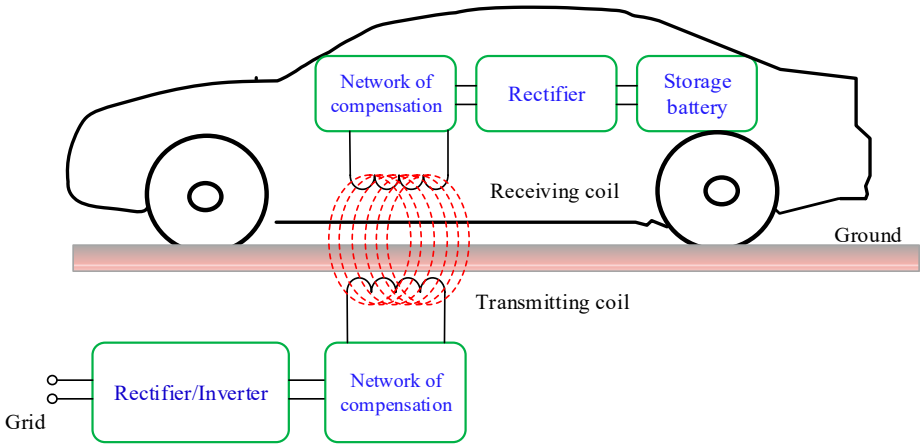

Figure 1. General wireless power transfer charging system for EVs.

To address the limitations of traditional wireless charging systems, particularly high EMI and E-field leakage, our study proposes the AVPC, which incorporates several innovative features. First, the AVPC's innovative coil configuration significantly reduces E-field emissions while maintaining the same power transfer as traditional coils, enhancing the system's operational reliability. Second, the AVPC's enhanced safety protocols primarily focus on minimizing EMI and E-field leakage, the main contributors to potential health risks associated with electromagnetic emissions. While the AVPC effectively reduces the E-field, it intentionally maintains the H-field (magnetic field) necessary for efficient power transfer, as the leakage magnetic field is not the primary concern in this study. The AVPC's ability to selectively reduce the E-field while maintaining the H-field is a key aspect of this research. Third, the AVPC demonstrates exceptional versatility and broad adaptability for various device applications, including EVs, mobile devices, and medical equipment, showcasing its potential beyond traditional applications.

Table 1 presents a detailed comparison of the AVPC and traditional coil designs, emphasizing the AVPC's significant improvements in E-field emission reduction [38], innovative current flow sequence, and broad adaptability to various devices while maintaining comparable energy transfer efficiency. Our experimental and simulation results demonstrate that the AVPC achieves an 85% reduction in E-field emissions compared to traditional coil designs while maintaining the same power transfer efficiency as traditional coils. These quantitative findings underscore the effectiveness of the AVPC in addressing the limitations of conventional wireless charging systems, positioning it as a superior solution for various wireless charging applications.

Table 1. Comparison of traditional coil and AVPC configuration.

Feature	Conventional Coil	AVPC
E-field emission reduction	Limited	Significantly improved
Energy transfer efficiency	High	Comparable to conventional coils
E-field neutralization method	Capacitors (complex)	Design configuration
Innovative current flow sequence	No	Yes
Sequential turn progression	Turns in sequence	Not applicable
Adaptability to various devices	Limited	Broad (EVs, mobiles, medical equipment)

The key objectives of this study are as follows:

1. Primary objective: Develop and validate the AVPC design, demonstrating its effectiveness in reducing EMI and E-field emissions while maintaining efficient power transfer, thus addressing the most pressing safety and performance issues in traditional wireless charging systems.
2. Experimental validation: Conduct comprehensive testing to measure the EMF emissions of the AVPC under various operating conditions and compare the results with those of traditional coil systems to quantify improvements in field management.
3. Safety and efficiency metrics: Assess the safety improvements brought by the AVPC, particularly through reduced EMF exposure, and analyze the system's efficiency in terms of power transfer and energy loss.
4. Design optimization: Explore new design variations of the AVPC based on the findings from the previous objectives, aimed at further enhancing its performance, safety, and compatibility with high-power wireless charging applications.

To experimentally validate the AVPC's enhanced capabilities, comprehensive testing will be conducted using advanced measurement techniques to assess the coil's efficiency and EMF emissions across various operational conditions. Additionally, simulations will be performed to investigate the impact of the AVPC's design on the system's performance and explore potential design optimizations.

The paper is structured as follows: Section 2, Proposed Coil Structure Compared to the Traditional Coil, presents the design methodology and developmental insights of the AVPC, contrasting it with traditional coil structures. Section 3, Simulation Analysis of the Coil, delves into comprehensive simulation studies to validate the performance of the AVPC. In Section 4, the paper transitions into the experimental validation, providing a detailed analysis of the experimental setup and discussing the results obtained from real-world testing scenarios. The paper culminates in Section 5, the conclusion, summarizing the key findings, drawing conclusions from both the simulated and experimental investigations, and offering perspectives for future research in EV wireless charging systems.

2. Proposed Coil Structure Compared to the Traditional Coil

2.1. Structural Design and Development of AVPC

This section elucidates the innovative design principles and structural characteristics of the AVPC, an innovative advancement in EV wireless charging technology. The AVPC's revolutionary design departs from conventional coil configurations by employing a unique turn sequencing pattern. In traditional coils, as shown in Figure 2a, the current flows sequentially through the turns in the order of L_1, L_2, L_3, L_4, L_5, and L_6. In contrast, the AVPC's electrical current follows a different path while maintaining the same direction of current flow. In the AVPC design depicted in Figure 2b, the current first flows through the odd-numbered turns L_1, L_3, and L_5 and then through the even-numbered turns L_2, L_4, and L_6. Similarly, in the AVPC design shown in Figure 2c, the current flows through L_1, L_3, and L_5, and then L_6, L_4, and L_2, maintaining the same direction of current flow throughout the coil. This innovative sequencing creates an alternating voltage pattern across the coil, with higher voltage differences between adjacent turns compared to traditional coils.

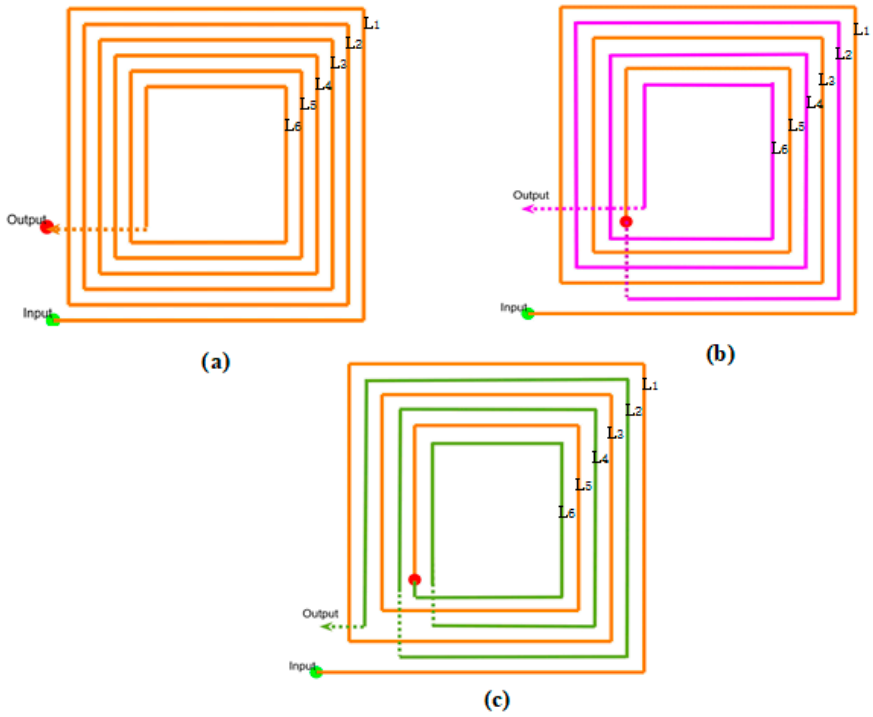

Figure 2. Structure of the coil prototype. (**a**) Traditional coil. (**b**) AVPC 1. (**c**) AVPC 2.

LTSpice simulations and mathematical analyses of the voltage distributions in the AVPC and traditional coil reveal a significant difference in their voltage patterns. In the AVPC, the voltage waveforms of adjacent turns exhibit a phase difference, when compared to the average voltage of the coil, which is used as the reference. This phase difference indicates substantial voltage differences between neighboring turns, resulting in alternating high and low voltage points along the coil. In contrast, the voltage waveforms of adjacent turns in the traditional coil are in-phase, suggesting a more uniform voltage difference distribution and smaller voltage differences between neighboring turns. The alternating voltage pattern created by the innovative sequencing in the AVPC design contributes to reduced field intensity in the vicinity of the coil, ultimately leading to a reduction in E-field emissions compared to traditional coil designs.

The design of the AVPC involves careful consideration of its geometry and parameters to optimize its performance. The key parameters that define the coil's geometry include the outer diameter D_{out}, inner diameter D_{in}, wire diameter d_w, and spacing between turns (s). These parameters are related to the number of turns (N) in the coil, as described by Equation (1):

$$N = \frac{(D_{Out} - D_{In})}{(2 \times d_w + 2 \times S)} \quad (1)$$

Equation (1) governs the relationship between the geometrical parameters and the number of turns in the coil. By carefully selecting these parameters, the geometry can be optimized while maintaining the same power transfer as traditional coils and achieving reduced E-field emissions, particularly in the case of AVPC.

The inductance of the coil (L) is calculated using Equation (2), where μ_0 is the permeability of free space ($4\pi \times 10^{-7}$ H/m), N is the number of turns, A is the cross-sectional area of the coil (m^2), and l is the length of the coil (m) [39]. The mutual inductance between adjacent turns (M) is given by Equation (3):

$$L = \frac{(\mu_0 \times N^2 \times A)}{l} \quad (2)$$

$$M = \frac{(\mu_0 \times N_1 \times N_2 \times A_m)}{L_m} \tag{3}$$

where N_1 and N_2 are the number of turns in adjacent coil segments, A_m is the effective cross-sectional area of the region where the magnetic fields of the adjacent segments interact, contributing to the mutual inductance effect, and L_m is the effective length of the mutual inductance path, representing the average distance between the adjacent coil segments contributing to the mutual inductance effect. The coupling coefficient between adjacent turns (k) is calculated using Equation (4), where M is the mutual inductance between adjacent turns and L_1 and L_2 are the self-inductances of the adjacent turns. The quality factor of the coil (Q) is given by Equation (5), where ω is the angular frequency $(2\pi \times f)$, L is the inductance of the coil, and R is the resistance of the coil. The skin depth of the wire (δ) is calculated using Equation (6), where ρ is the resistivity of the wire material $(\Omega{\cdot}\mathrm{m})$, f is the frequency of the alternating current (Hz), and μ is the magnetic permeability of the wire material (H/m).

$$K = \frac{M}{\sqrt{L_1 - L_2}} \tag{4}$$

$$Q = \frac{(\omega \times L)}{R} \tag{5}$$

$$\delta = \sqrt{\frac{\rho}{\pi \times f \times \mu}} \tag{6}$$

The AVPC's structural uniqueness lies in its strategic arrangement of the turn sequence, which harnesses the principle of electric field opposition. This design involves an innovative Sequential Inversion Winding (SIW) technique where the current flows through the turns in a specific sequence that creates an alternating voltage pattern across adjacent turns. Unlike traditional coil designs, where the voltage phases of adjacent turns are the same, leading to additive electric fields, the AVPC design arranges the turns such that the voltage potentials between adjacent turns are effectively out-of-phase. While direct measurements of the voltages (e.g., V_1 and V_2) at each turn might show them as in-phase due to the same AC source, the relative voltage differences between adjacent turns in the AVPC design create effective phase shifts. These phase shifts are determined by using the average voltage of the coil and extracting the voltages of individual nodes from this average voltage. By comparing the extracted node voltages, the phase shifts between adjacent turns can be clearly identified. Although each turn receives the same AC signal, the spatial arrangement and alternating voltage patterns cause adjacent turns to have voltages that effectively cancel each other out corresponding to the average voltage of the coil. This phase opposition results from the specific sequencing of the turns and the inherent geometric configuration of the coil. The cancelation effect can be described by the principle of superposition of electric fields. If E_1 and E_2 are the electric fields generated by adjacent turns with opposing voltages, the resultant electric field E_{Total} is given by the following:

$$E_{Total} = E_1 + (-E_2) \tag{7}$$

where E_1 is the electric field generated by one turn and $-E_2$ is the electric field generated by the adjacent turn with an opposite voltage polarity, effectively canceling out E_1. By optimizing the AVPC's design parameters, such as the number of turns, spacing between turns, and coil dimensions, this ingenious design feature enables the AVPC to significantly mitigate electromagnetic interference without relying on complex shielding or extensive modifications, ultimately simplifying the coil's architecture while enhancing its performance.

The AVPC's superior characteristics, as outlined in Table 1, position it as an environmentally friendly and user-safe solution, surpassing the limitations of conventional coil designs. The development of the AVPC represents a significant stride in addressing the pressing need for safer and more efficient wireless charging solutions. By reimagining the fundamental structure and voltage pattern of the coil, this innovative design paves the

way for overcoming persistent challenges in the field, setting a new paradigm for future advancements in EV wireless charging technology.

2.2. Simulation Setup and Preliminary Results

The simulation parameters and outcomes, depicted in Figures 3 and 4, play a vital role in validating the operational advantages of the AVPC design. The coil parameters (inductance and coupling coefficients) presented in Figure 4 and Table 2 are derived from the ANSYS FEM simulation of the coil pad structure shown in Figure 3a. LTSpice simulations were conducted using these data for both the AVPC (Figure 3c) and the traditional coil (Figure 3b), focusing on a six-turn configuration to simplify the analysis and understand the reason behind the E-field reduction.

To maintain accuracy while simplifying the analysis, assumptions such as ideal component behavior were made in the SPICE simulations. These assumptions allow for a focused study on the fundamental behavior of the AVPC design compared to the traditional coil structure.

Table 2. Coil inductance and system parameters.

Coil	Inductance (uH)	Parameter	Value
L_1	0.120	Input AC current I	5 A
L_2	0.087469	Resonant frequency	85 KHz
L_3	0.060760	Shielding plate	74 mm × 74 mm × 1 mm
L_4	0.043119	Ferrite core 1	72 mm × 72 mm × 2 mm
L_5	0.030174	Coil dimension	70 mm × 70 mm × 3 mm
L_6	0.019673	Coil turn to turn spacing	1.5 mm

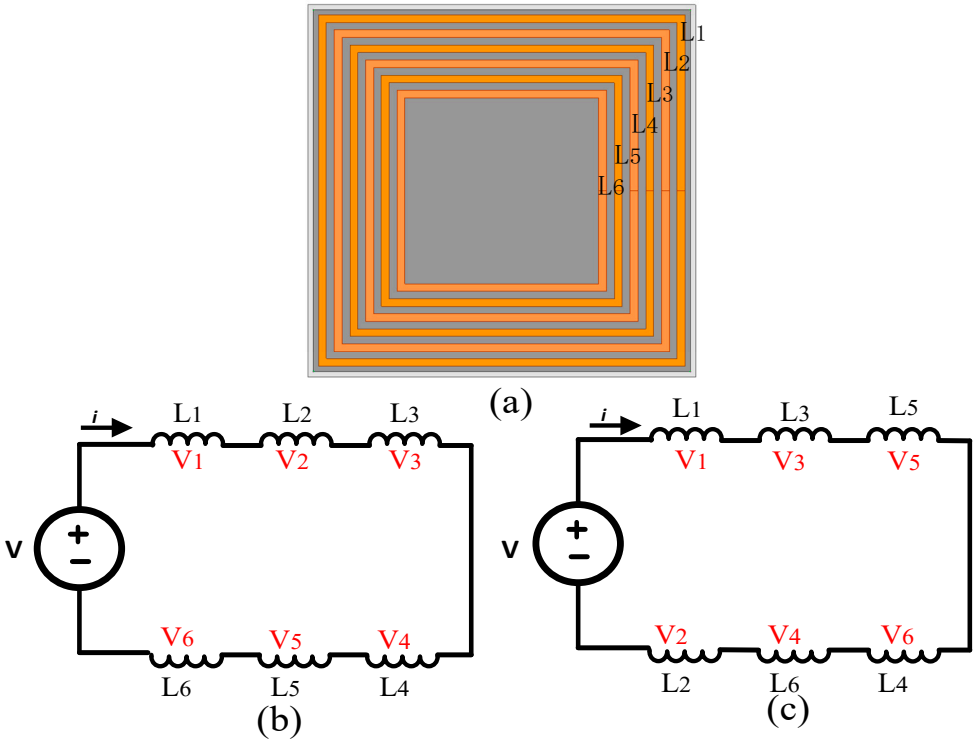

Figure 3. E-field mitigation in wireless charging systems. (**a**) Optimized coil design. (**b**) Spice circuit of traditional coil. (**c**) Spice circuit of the AVPC.

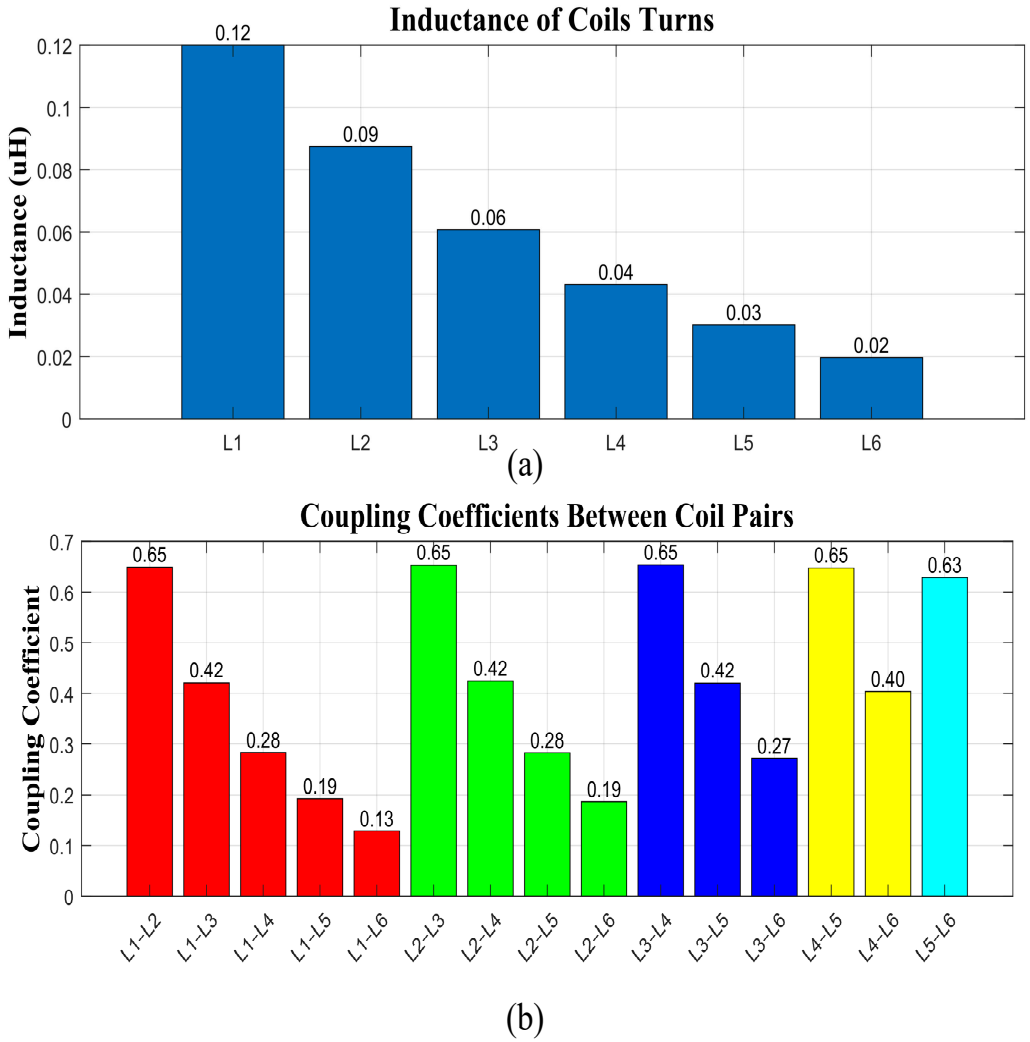

Figure 4. Coil Parameter. (**a**) Inductance. (**b**) Coupling coefficient.

As illustrated in Figure 3b,c, the traditional coil features a sequential arrangement, while the AVPC design employs an alternating coil arrangement to strategically reduce E-field emissions. The LTSpice simulations, measuring average voltage waveforms at different nodes, highlight the role of phase differences in the AVPC's E-field reduction capability. This comprehensive analysis of the voltage distribution and phase differences between the two designs demonstrates the AVPC's superior ability to suppress E-field emissions. The AVPC's unique configuration enhances E-field mitigation through phase differences and field cancelation, resulting in superior performance compared to the traditional coil while maintaining comparable power transfer.

2.3. Waveform Analysis and E-Field Mitigation through Spice Simulation

The voltage waveforms of the traditional and AVPC coil designs, obtained from SPICE simulations and presented in Figure 5a,b, are essential for understanding their electrical characteristics and inferring potential E-field emissions. The simplified equation $E = (V_{total}/2\pi\varepsilon_0 r)$ demonstrates how the total voltage across the coil correlates with the E-field strength. In the traditional coil design, the in-phase voltage waveforms across inductors L_1 to L_6, described by the relationship $V_i = J\omega L_i I_i$, enhance magnetic field generation, but also increase the potential for E-field emission due to the higher total voltage across the coil, which can be expressed as the sum of the voltages across each inductor.

$$V_{total} = V_1 + V_2 + \cdots + V_n \tag{8}$$

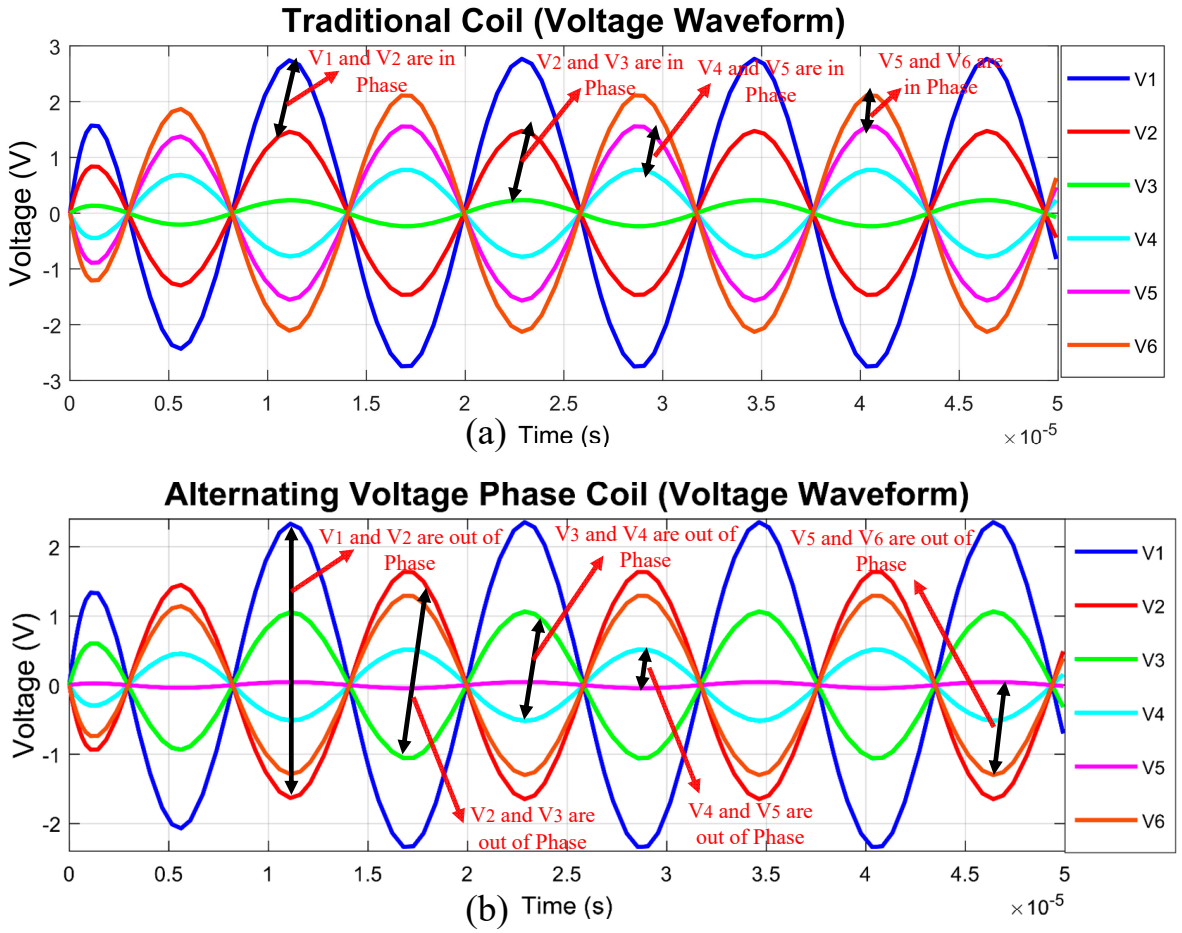

Figure 5. Coil wave forms. (**a**) Traditional coil. (**b**) AVPC.

In contrast, the AVPC design introduces a strategic phase shift to mitigate E-field emissions. The modified equation $V_i = J\omega L_i I_i - J\omega M_{ik} I_k$, where M_{ik} represents the mutual inductance between adjacent turns, leads to a phase shift between the voltages across adjacent turns, promoting phase opposition and reducing the total voltage and, consequently, the E-field emissions. The total voltage across the coil in the AVPC design can be expressed as the sum of the voltages across each inductor, considering the phase shift.

$$V_{total} = V_1 + V_2 e^{(j\theta_2)} + \cdots + V_n e^{(j\theta_n)} \tag{9}$$

The 180 degree phase shift is achieved through the specific arrangement and sequencing of the turns in the AVPC design, where the strategic placement of turns with respect to each other promotes the desired phase opposition. The formula used in the SPICE simulation is shown in Equation (12) and demonstrates how the voltages at different nodes are averaged, leading to an effective phase shift. This analysis reveals the phase difference in the voltage in the AVPC compared to the traditional coil, as shown in Figure 5a,b.

The average voltage across the turn is calculated as follows:

$$V_{avg} = \frac{1}{N} \sum_{i=1}^{N} V_i \tag{10}$$

The effective voltage at a specific turn, say V_i, is given by the following:

$$V_{effective} = V_1 - V_{avg} \tag{11}$$

The generalized form of the voltage at any turn V_{turn} is as follows:

$$V_{turn} = V_{turn} - \frac{1}{N}\sum_{i=1}^{N} V_{all\ turns} \tag{12}$$

Figure 5 illustrates the voltage waveforms for the traditional coil and the AVPC. In the traditional coil design (Figure 5a), the in-phase voltage waveforms V1 and V2 have positive peaks reaching approximately 2.8V, leading to higher overall voltage and potentially increased E-field emissions. Conversely, the AVPC design (Figure 5b) exhibits an out-of-phase relationship between V1 (positive peaks around 2.4 V) and V2 (negative peaks around −2.4 V), resulting in lower overall voltage and reduced E-field emissions. The E-field strength at a distance r from the coil can be approximated using Equation (13).

$$E = \frac{(V_{total})}{(2\pi\varepsilon_0 r)} \tag{13}$$

where V_{total} represents the total voltage across the coil and ε_0 is the permittivity of free space (8.85×10^{-12} F/m). This Equation provides a simplified estimation of the E-field strength based on the total voltage and the distance from the coil [40]. However, as presented in [41,42], a more detailed analysis of the E-field distribution is necessary to fully understand the electromagnetic behavior of these coil structures and accurately compare the E-field mitigation capabilities of the AVPC and traditional coil designs.

The LTSpice circuit model, based on the AVPC design, facilitates the desired phase cancelation through the innovative arrangement of coil turns, concentrating the magnetic field for efficient energy transfer while substantially diminishing E-field emissions. The essential difference between the two designs lies in the phase relationship between the voltages, with the AVPC demonstrating an out-of-phase relationship that enables E-field mitigation while maintaining energy transfer. This is achieved by ensuring that the current through the coil remains consistent, thereby sustaining the magnetic field necessary for energy transfer. Simulation results confirm the AVPC's enhanced ability to achieve a balance between energy transfer efficiency and E-field mitigation by leveraging phase shift cancelation to reduce E-field emissions while preserving core functionalities, setting a new standard in wireless charging technology that prioritizes both electromagnetic compatibility and safety.

3. Simulation Analysis of the Coil

3.1. Simulation Parameters and Setup

Finite Element Method (FEM) simulations, performed using a computational electromagnetics software package, were used to analyze the electromagnetic properties of the traditional coil and AVPC designs in EV wireless charging systems. Table 3 lists the key simulation parameters, including input current, resonant frequency, and dimensions of the shielding plate, ferrite core, and coil, which are selected to represent realistic operating conditions in EV wireless charging applications. While Table 2 focuses on the specific case of a six-turn coil to simplify the analysis and understand the E-field reduction mechanism, Table 3 provides a more comprehensive set of simulation parameters to evaluate the performance of the traditional coil and AVPC designs under various operating conditions. These simulation parameters were then used as a basis for the experimental setup to ensure consistency between the computational models and the physical prototype.

The FEM simulations discretize the domain using second-order tetrahedral elements and apply appropriate boundary conditions to represent the wireless charging pad, an essential component of the EV wireless charging system. The pad is modeled with realistic dimensions, materials, and operating conditions to accurately capture its electromagnetic

behavior. The electromagnetic responses, such as magnetic field distribution, electric field intensity, and power transfer capability, are computed by solving Maxwell's equations iteratively. By accurately modeling the pad's electromagnetic properties, the FEM simulations provide valuable insights into the performance and safety aspects of the EV wireless charging system.

Table 3. System parameters of pad.

Parameters	Values
Input AC current	5 A
Resonant frequency	85 KHz
Shielding plate dimension	420 mm × 420 mm × 4 mm
Ferrite core dimension	404 mm × 404 mm × 5 mm
Coil dimension	400 mm × 400 mm × 2.5 mm
Number of turns	22 Turns
Coil inductance	336.4 uH

Key performance metrics, such as peak magnetic field strength, average electric field intensity, and power transfer capability, are extracted from the simulation results and compared between the traditional coil and AVPC designs. Visualizations of field distributions and current densities provide insights into the electromagnetic behavior of the coils. The FEM simulations offer a comprehensive assessment of the electromagnetic performance of AVPC designs compared to traditional coil setups, contributing to the understanding of their potential in enhancing the safety and capability of EV wireless charging systems.

3.2. Electromagnetic Field Distribution and the Impact of Conductive Materials

A comparative analysis of electromagnetic field distributions, focusing on electric field (E-field) emissions for both traditional and AVPC designs, demonstrates the AVPC's enhanced effectiveness in E-field mitigation. As demonstrated in Figure 6, the E-field intensity around the traditional coil is noticeably higher compared to the AVPC models, which exhibit a significant reduction in E-field intensity. This reduction is quantitatively supported by the data presented in Figure 7, where the AVPC designs consistently show lower E-field intensities at various measurement points.

The FEM analysis clearly illustrates the AVPC's ability to reduce E-field emissions, emphasizing a pivotal advancement in coil technology aimed at safer wireless charging solutions. This consistent reduction in E-field level underscores the AVPC's effectiveness in mitigating electromagnetic emissions across a wide spatial distribution.

Simulations were conducted with a foreign metal object (FMO) positioned 100 mm above the coils to mimic practical conditions in electric vehicle (EV) charging scenarios. Figure 8 illustrates the influence of the FMO on the E-field distribution for each coil design.

The presence of the FMO led to an increase in E-field intensity across all designs due to the metal's interaction with the electromagnetic fields. However, the AVPC configurations demonstrated remarkable resilience by suppressing the amplification of E-field levels. The AVPC 2 design demonstrates exceptional performance, maintaining significantly lower E-field intensities compared to the traditional coil at all measurement points, even in the presence of the FMO (Figure 7b).

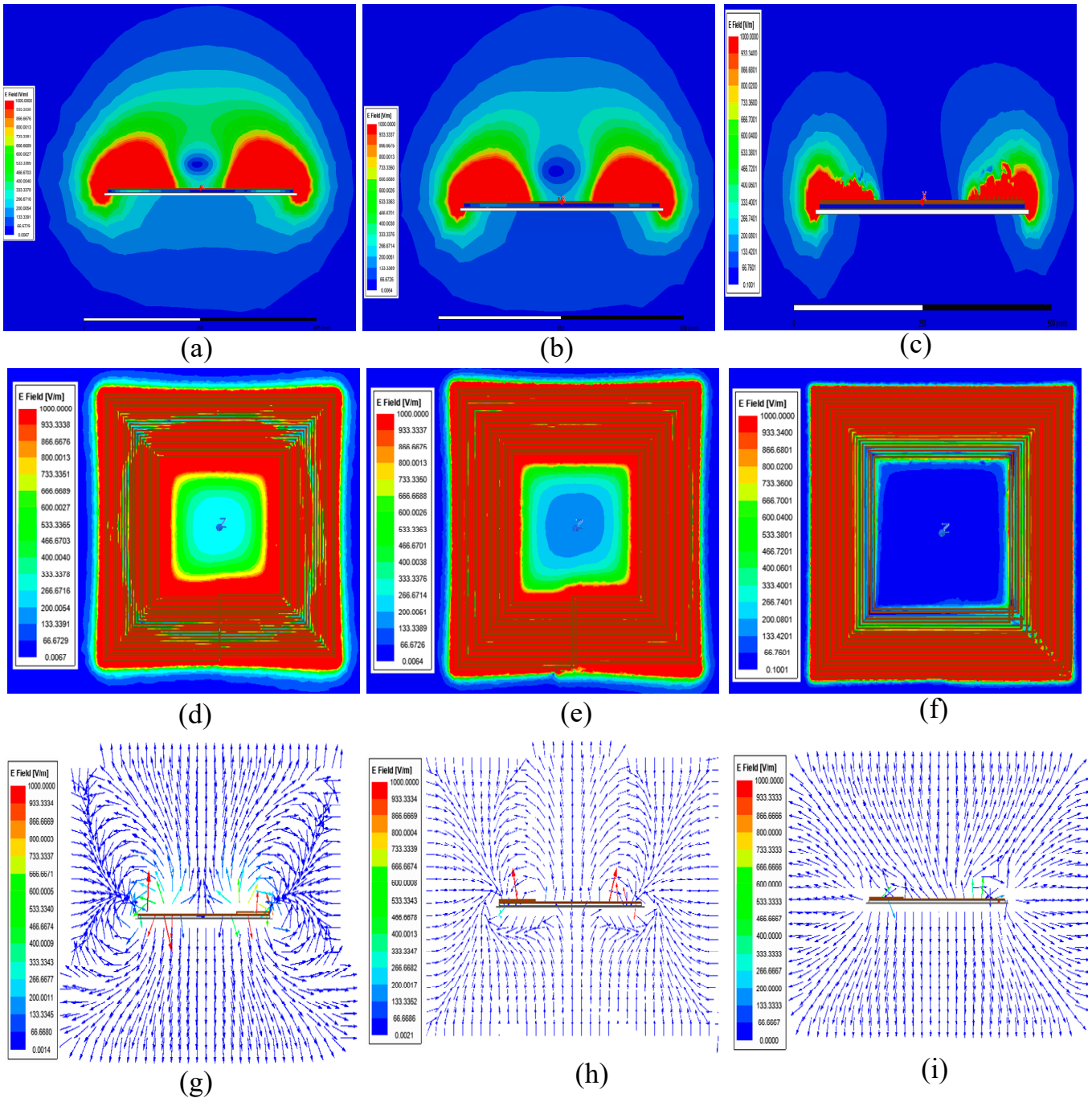

Figure 6. Comparative E-field distributions in coil designs without environmental effects. (**a**) Traditional coil side view. (**b**) AVPC 1 side view. (**c**) AVPC 2 side view. (**d**) Traditional coil top view. (**e**) AVPC 1 top view. (**f**) AVPC 2 top view. (**g**) Traditional coil side view vector distribution. (**h**) AVPC 1 side view vector distribution. (**i**) AVPC 2 side view vector distribution.

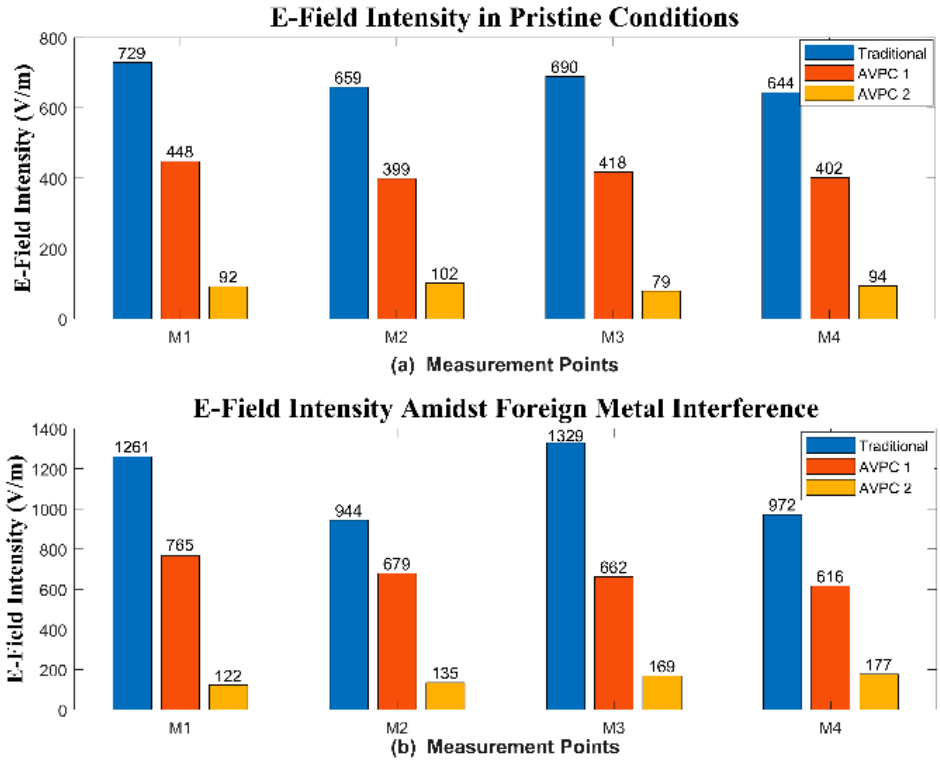

Figure 7. E−field intensity comparison at measurement points at 100 mm distance at Z axis. (**a**) E−Field Intensity in Pristine Conditions (**b**) E-Field Intensity Amidst Foreign Metal Interference.

3.3. Evaluating Electric Field Mitigation and Similar Magnetic Field Distribution in Coil Design

Figure 7 presents a detailed comparison of electric field (E-field) intensities measured at specific points, illustrating the effectiveness of the AVPC designs in managing electromagnetic fields under various conditions. The measurement points M1 (X = 0, Y = 120, Z = 100 mm), M2 (X = 0, Y = 160, Z = 100 mm), M3 (X = 0, Y = −120, Z = 100 mm), and M4 (X = 0, Y = −160, Z = 100 mm) are strategically located at different coordinates. Figure 7a provides baseline E-field measurements at a 100 mm distance along the Z-axis in an environment free from external influences, while Figure 7b reveals the E-field intensities in the presence of foreign metal objects, demonstrating the robust capability of the AVPC designs to mitigate E-field disturbances.

The AVPC designs, particularly AVPC 2, demonstrate a significant reduction in E-field intensities across all measurement points. Under pristine conditions (Figure 7a), the AVPC 2 design exhibits significantly lower E-field intensities compared to the traditional coil at each measurement point, showcasing its effectiveness in mitigating electromagnetic emissions across a wide spatial distribution. Moreover, despite the interference caused by conductive materials, the AVPC configurations, especially AVPC 2, consistently maintain their superior E-field mitigation performance, as evidenced by the results presented in Figure 7b. This reduction in E-field levels under both pristine and interfering conditions underscores the robustness of the AVPC designs in managing electromagnetic emissions.

The comparative analysis of the magnetic field distribution in the traditional coil and two AVPC designs, as depicted in Figure 9, reveals a similar magnetic field distribution within each coil design. The consistent color patterns indicate that the magnetic field intensity and distribution are comparable across all three designs, particularly in the central regions where the intensity is strongest. This similarity in patterns suggests that the AVPC designs maintain a magnetic field distribution that closely resembles that of the traditional coil.

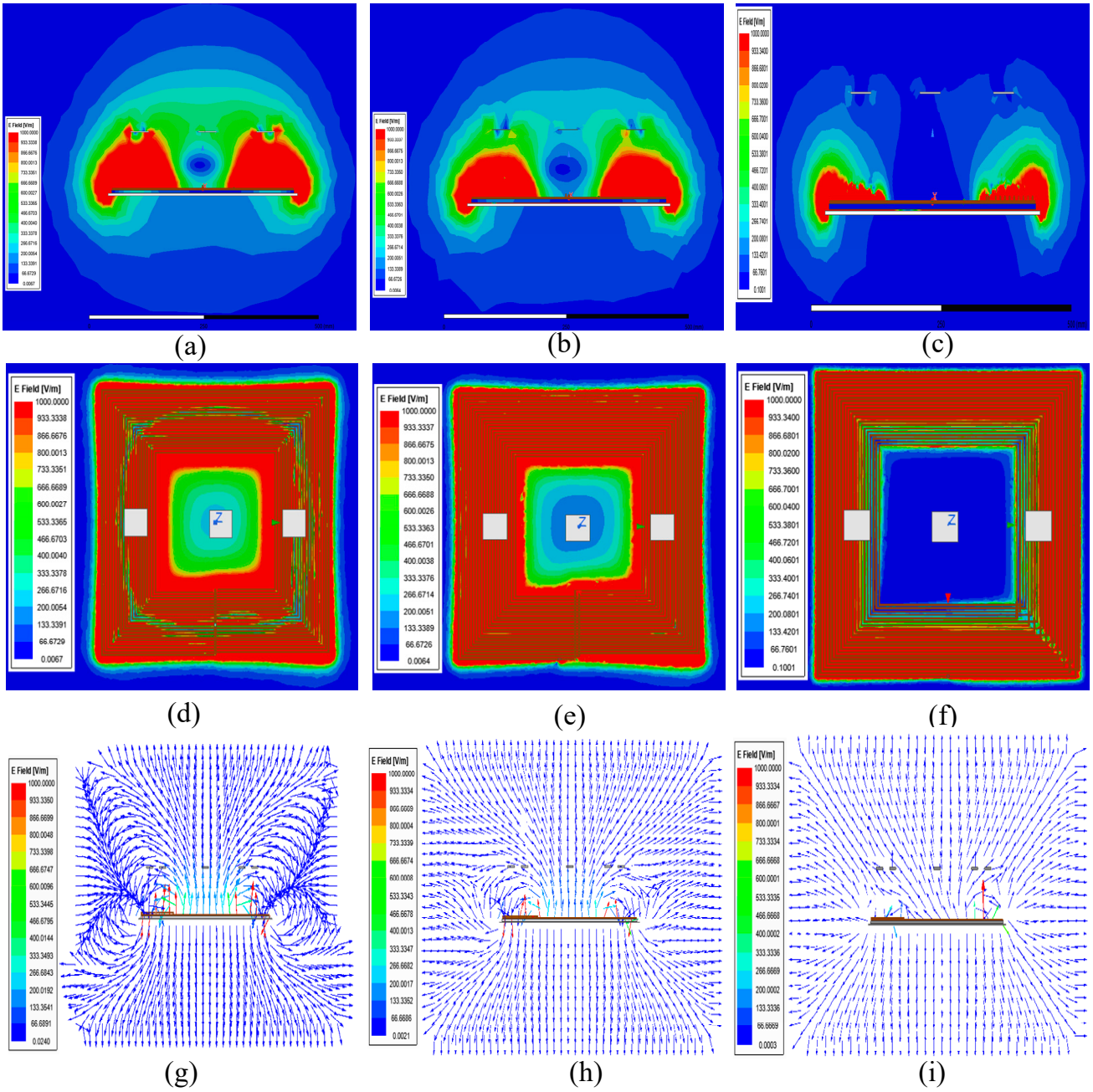

Figure 8. Comparison E-field distribution with a conductive aluminum plate at 100 mm distance. (**a**) Traditional coil side view. (**b**) AVPC 1 side view. (**c**) AVPC 2 side view. (**d**) Traditional coil top view. (**e**) AVPC 1 top view. (**f**) AVPC 2 top view. (**g**) Traditional coil side view vector distribution. (**h**) AVPC 1 side view vector distribution. (**i**) AVPC 2 side view vector distribution.

Observing similar magnetic field distributions across different coil configurations suggests that the AVPC designs can maintain a magnetic field comparable to the traditional coil. This analysis indicates that the enhancements made to reduce E-field emissions in AVPC designs do not significantly alter the magnetic field distribution, which is favorable for maintaining the effectiveness of power transfer while minimizing electromagnetic exposure through innovative coil design.

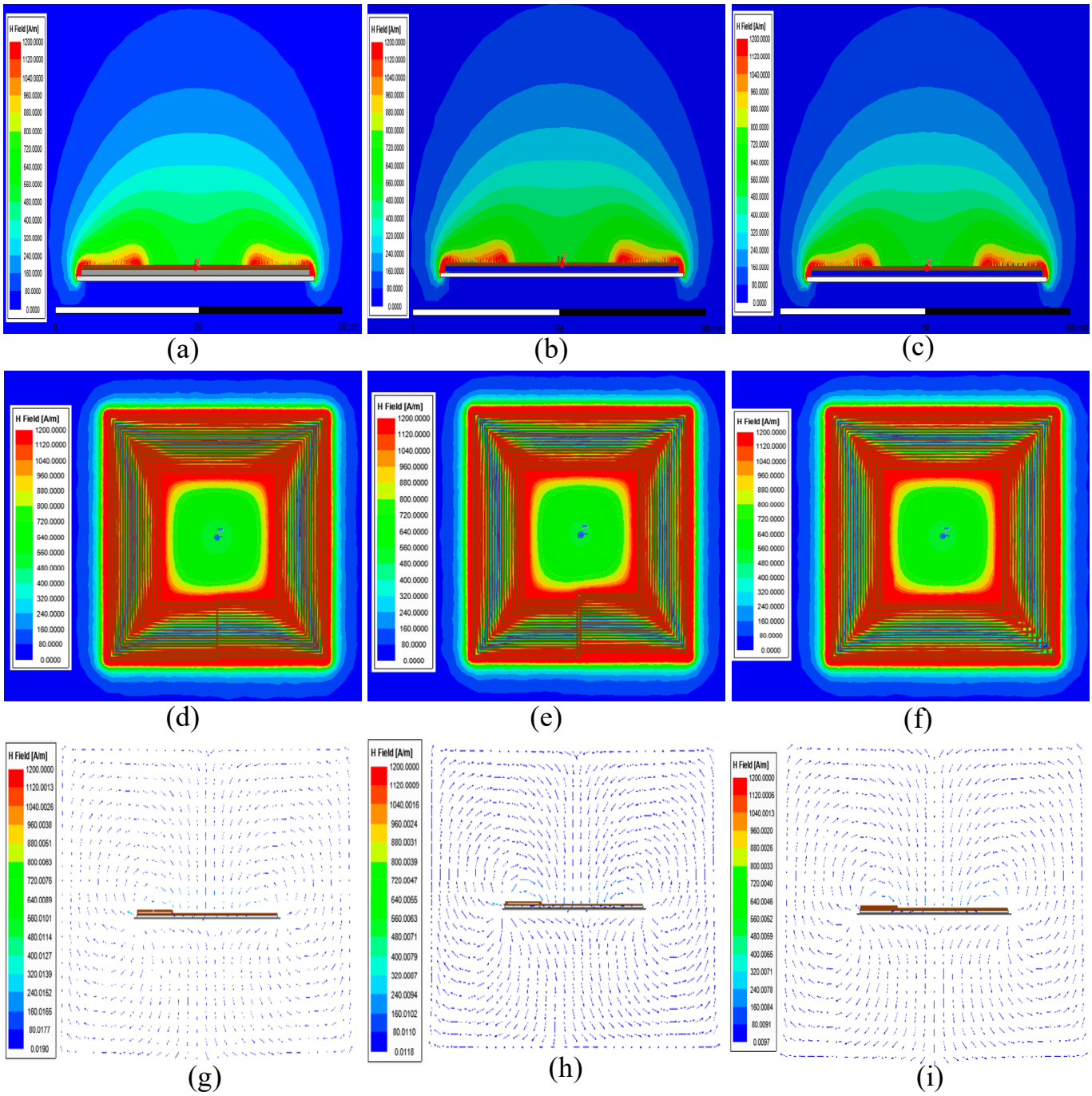

Figure 9. Comparison of the H-Field in the design coil paid. (**a**) Traditional coil side view. (**b**) AVPC 1 side view. (**c**) AVPC 2 side view. (**d**) Traditional coil top view. (**e**) AVPC 1 top view. (**f**) AVPC 2 top view. (**g**) Traditional coil side view vector distribution. (**h**) AVPC 1 side view vector distribution. (**i**) AVPC 2 side view vector distribution.

4. Experimental Setup of Coil Design and Result Verification

4.1. Methodical Assessment and Verification of Coil Design Performance

The practical performance of the innovative AVPC designs was thoroughly evaluated in a laboratory setting that closely mimicked real-world conditions to enhance safety and efficiency in electric vehicle wireless charging applications. Extensive testing simulated real-world EV charging conditions in a laboratory setting, comparing traditional coils against AVPC configurations, as shown in Figure 10. The experiments were conducted using three coils of identical size, number of turns, frequency, and input current for each

design (traditional, AVPC 1, and AVPC 2). Each coil was tested to ensure the reliability and reproducibility of the results. The traditional and AVPC coils were energized using an AC source to mimic typical charging behaviors, with an NF-5035 spectrum sensor placed 100 mm above the coil to closely resemble the spacing in practical EV charging scenarios for accurate E-field data collection.

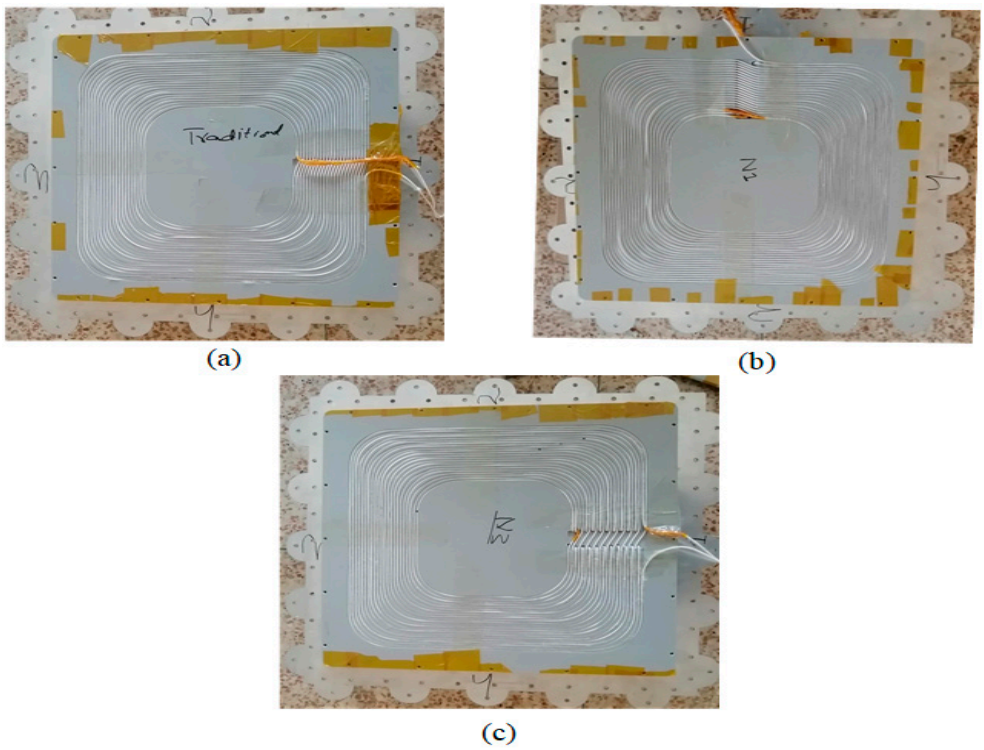

Figure 10. Comparative analysis of electromagnetic radiation distributions in innovative coil designs. (**a**) Traditional coil. (**b**) AVPC 1. (**c**) AVPC 2.

The NF-5035 spectrum sensor was selected for its proficiency in detailed electromagnetic detection, providing an accurate representation of EV charging scenarios. This enabled a focused analysis of the coils E-field emissions, specifically isolating the AVPC's inherent electromagnetic attributes. The collected data revealed that AVPC 1 and AVPC 2 designs exhibited a reduction in average E-field emissions as compared to the traditional coil design. Observations were systematically analyzed to identify the compliance and the distinct advantages of the AVPC design.

The experimental setup, depicted in Figure 11, maintained a consistent 100 mm distance between the coil and sensor to generate reliable and comparable data on electric field emissions from different coil designs. The E-field measurements were recorded at four different points around each coil, showing the variation but while still being comparable to the traditional coil, demonstrating the reduction in the E-field in the AVPC designs.

The AVPC employs an LCC compensation network to adjust the phase across the coil, facilitating optimal electromagnetic field interaction and E-field mitigation. While the LCC topology is used in experiments to validate the design, it is important to note that the inherent 180 degree phase shift primarily arises from the coil geometry itself, not the LCC network. Different topologies, such as series–series, series–parallel, parallel–series, and parallel–parallel, can be used, as the phase shift depends on the coil geometry rather than these topologies [43]. The phase shift, calculated using Equation (14), is essential for neutralizing fields emitted by adjacent turns, enhancing E-field mitigation.

$$\phi = \arctan\left(\frac{Imaginary(z)}{Real(z)}\right) \tag{14}$$

Ensuring that the compensation network resonates at the coil system's natural frequency, calculated using Equation (15), is essential for efficient energy transfer and preserving the geometrically induced phase shift.

$$f_0 = \frac{1}{2\pi\sqrt{LC}} \tag{15}$$

The deliberate incorporation of the LCC compensation network was essential in the experimental methodology, providing precise control over the electric field generated by the coil. While the experimental setup closely mimics real-world EV charging conditions, future research should focus on validating the AVPC's performance in actual EV charging scenarios to further strengthen this study's findings.

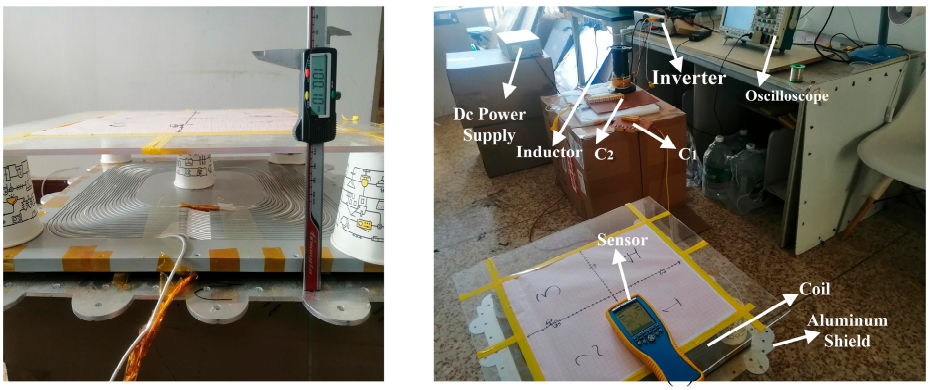

Figure 11. Shows experimental setup illustrating LCC compensation network and measurement apparatus. (**a**) Show distance between coil and the measuring points. (**b**) Experimental setup and equipment's.

4.2. Detailed Analysis of E-Field Emission Findings

The experimental study quantified the E-field emissions of both traditional and AVPC designs to compare their performance in reducing E-field radiation. The NF-5035 spectran sensor designed by aaronia AG, a German company in gewerbegebiet aaronia AG was used to measure E-field levels accurately, replicating typical EV charging scenarios. The measurement points were located at a height of 100 mm above the coil surface, with specific coordinates of (x = 0 mm, y = 120 mm, 160 mm, −120 mm, −160 mm) for each coil design. These locations were selected based on the high E-field intensities observed in the simulations (Figures 6 and 8), corresponding to regions where the E-field is expected to be the strongest. This allows for a comprehensive assessment of the AVPC designs' performance in mitigating E-field radiation. The simulations also guided the experimental setup by considering the impact of nearby conductive objects, such as an aluminum plate, on the E-field's distribution.

Figure 12 illustrates the specific measurement points on each coil design, providing a visual representation of the locations where E-field data were collected. The arrows in Figure 12a–c indicates the four strategic points around the traditional coil, AVPC 1, and AVPC 2, respectively, where the E-field measurements were recorded.

The experiments were conducted in a normal laboratory setting to maintain a realistic environment. However, variability in E-field readings was observed within specific ranges. This variability can be attributed to environmental factors, such as the presence of nearby metallic objects or electromagnetic interference from other devices, which are relevant to the European Directive limit for public human exposure to EMF at 85 kHz, set at 87 V/m. The presence of such factors in real-world EV charging scenarios could potentially impact the performance and safety of the charging system. To mitigate these effects, strategies such as shielding, adaptive control systems, site planning, and continuous monitoring can

be implemented. These measures aim to ensure stable and safe charging conditions, even in the presence of environmental influences. Notably, the AVPC designs exhibited lower fluctuations compared to the traditional coil, suggesting better environmental adaptability.

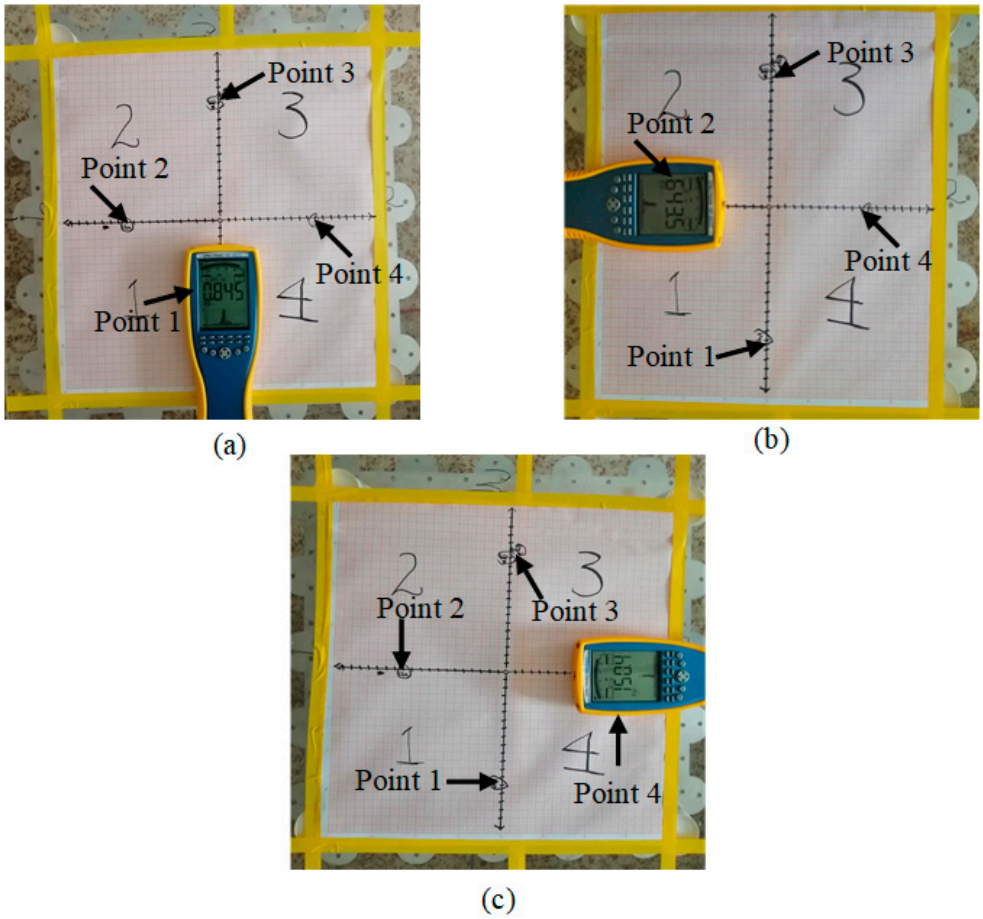

Figure 12. Measurement E-field emission comparisons across coil designs. (**a**) Traditional coil. (**b**) AVPC 1. (**c**) AVPC 2.

4.3. Quantitative Assessment of E-Field Mitigation in AVPC Designs

The simulation results shown in Figure 7 provided initial insights into the distribution, which were further supported by the experimental findings illustrated in Figure 13, demonstrating the strong correlation between the simulated and measured data. Figure 13 presents the corresponding E-field data collected from these measurement points, enabling a comparative analysis of the E-field intensity across the different coil designs. The graph clearly demonstrates the significantly lower E-field values observed across all measurement points for AVPC designs, particularly AVPC 2, compared to the traditional coil, highlighting the importance of minimizing E-field intensities in wireless charging solutions to reduce the overall cumulative exposure. This quantitative assessment highlights the effectiveness of the proposed AVPC designs in reducing E-field radiation. The experimental setup closely mimicked real-world EV charging conditions; however, measuring E-field values at specific points within a complete EV body structure can be challenging. Simulations are often used to obtain these measurements.

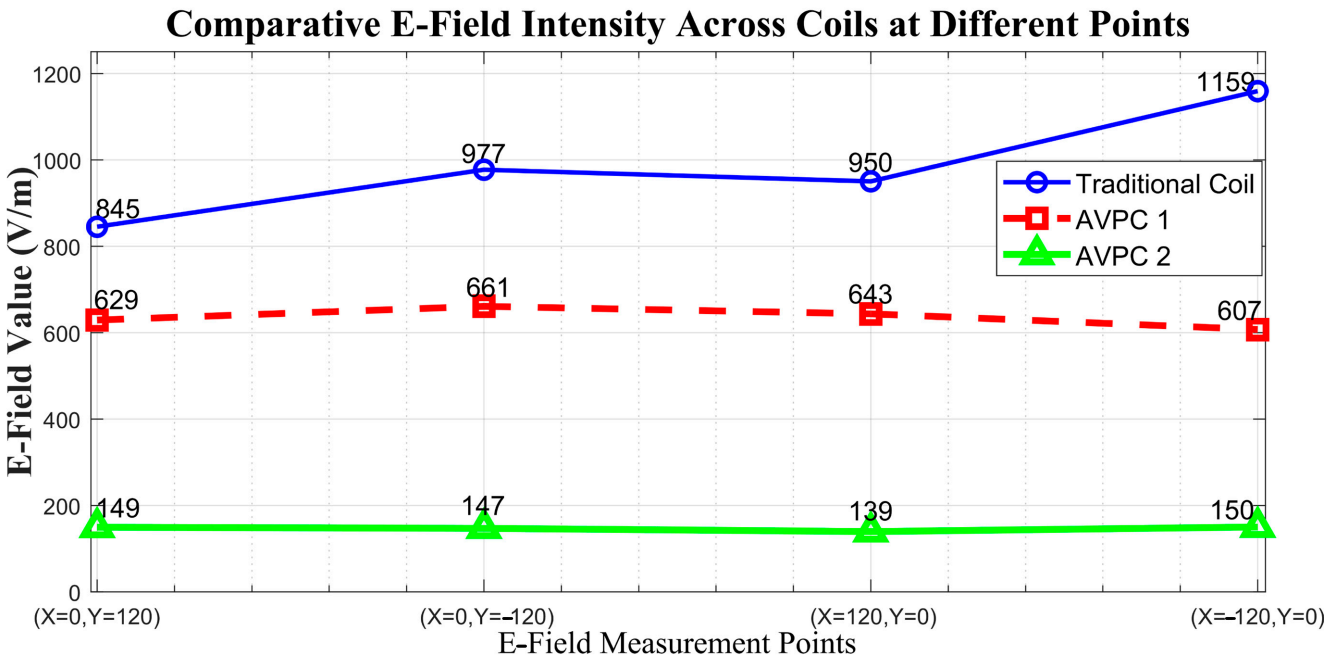

Figure 13. Comparative visualization of E−field intensity reduction across coil designs in EV charging applications.

To provide a comprehensive view, Figure 14 presents the average E-field intensities under different conditions for each coil configuration. The conditions evaluated include scenarios without an environmental effect (Without FMO), as well as those with an environmental effect introduced by the presence of foreign metal objects (With FMO). Practical experimental results were also considered, providing a triangulated approach to understanding E-field behavior in varying environmental contexts, including the presence of conductive materials like vehicle bodies. This understanding essential for the widespread adoption and public acceptance of wireless charging technology, particularly in the automotive industry.

In the absence of foreign metal objects, the traditional coil exhibits an E-field intensity of 680.5 V/m, serving as our reference point. Alternating voltage phase coils show a significant reduction in E-field intensity, registering at 416.8 V/m and 91.8 V/m, respectively. AVPC 1 achieved a notable reduction of 38.8%, while AVPC 2 demonstrated an impressive 86.5% reduction compared to the traditional design. Such marked reductions underscore the efficacy of the novel coil designs in mitigating E-field exposure, an important consideration for maintaining electromagnetic compatibility and ensuring user safety. When foreign metal objects are introduced, simulating a common environmental effect in electric vehicle (EV) wireless charging scenarios, we observe an overall increase in E-field intensity across all coil designs, highlighting the influence of conductive materials in proximity to the coils, an important variable in the design and deployment of wireless charging infrastructure. Despite this increase, the AVPCs continue to maintain lower E-field levels than the traditional coil, with AVPC 2 in particular showing resilience to the environmental change, increasing to 150.8 V/m but still remaining significantly lower than the traditional coil.

The experimental results validate the trends observed in simulated conditions, with AVPC1 and AVPC 2 exhibiting reduced E-field intensities of 635.3 V/m and 144.3 V/m, respectively. The close alignment between the experimental and simulated data affirms the reliability of our simulation model and reinforces the potential of AVPC designs in real-world applications. The findings underscore the importance of considering environmental factors, such as the presence of foreign metal objects and the distance between the transmitter coil and these objects in the design and implementation of wireless power transfer systems. These factors are particularly relevant in the context of the European Directive

limit for public human exposure to EMF at 85 kHz, set at 87 V/m. By significantly reducing E-field emissions, AVPC offers a safer and more environmentally friendly alternative to traditional coil designs, successfully meeting our central research aim of enhancing the safety and compatibility of wireless charging systems and propelling advancements in EV charging technology. The experimental findings demonstrate the AVPC's potential for practical implementation in EV wireless charging systems. However, several challenges need to be addressed for widespread adoption, including the integration with existing EV charging infrastructure, the development of standardized testing protocols, and the assessment of long-term reliability and durability under various environmental conditions.

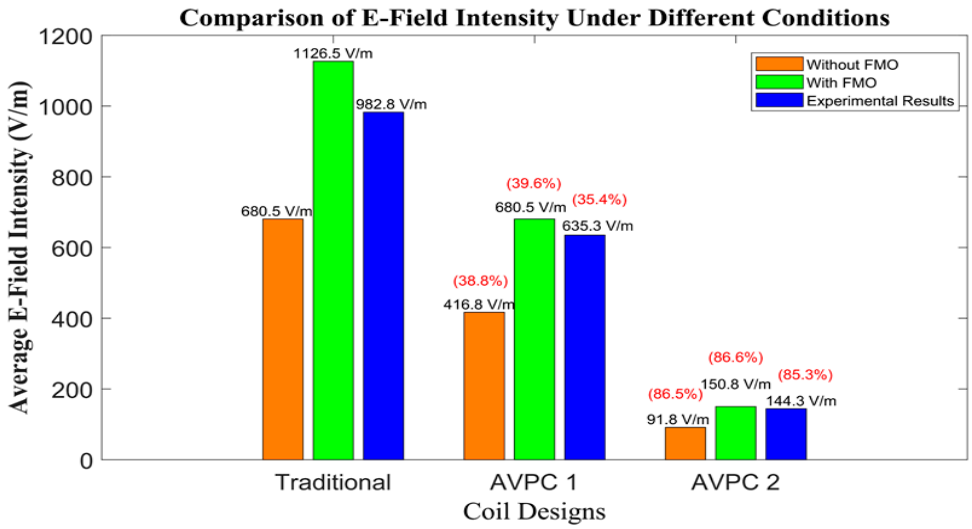

Figure 14. Average electric field intensities comparison.

5. Conclusions

In this paper, we presented the Alternating Voltage Phase Coil (AVPC), a novel coil design that effectively mitigates electromagnetic interference (EMI) in electric vehicle (EV) wireless charging systems. The AVPC's innovative geometry and current flow pattern, achieved through the Sequential Inversion Winding (SIW) configuration, significantly reduce E-field emissions by 85% while maintaining efficient power transfer comparable to traditional coils. The findings of this study clearly demonstrate the efficiency of the AVPC in reducing electric field intensity, an important factor for safer electromagnetic applications.

Comprehensive simulations and experimental validations establish that the strategic modifications in AVPC's turn geometry significantly mitigate E-field exposure, even in environments with foreign metal objects, enhancing electromagnetic compatibility. These results validate the AVPC as a promising approach for developing electromagnetic systems with stringent safety requirements.

The AVPC's adaptability to various devices underscores its broad applicability across multiple industries. This research contributes to the fundamental understanding of electromagnetic field behavior in wireless power transfer systems and opens up new avenues for optimization and innovation. Future work will focus on further enhancing the AVPC's performance, investigating alternative materials, and exploring its scalability for higher power applications.

The AVPC represents a significant advancement in EV wireless charging technology, offering a safer, more efficient, and eco-friendly solution. Future research should focus on validating the AVPC's performance in actual EV charging scenarios to further strengthen the study's findings and support the widespread adoption of this innovative technology. These findings provide a solid foundation for future research and development in designing more efficient and safer coil configurations, with the potential for widespread industrial application and integration. The AVPC is a highly important innovation that plays a vital

part in ensuring conformity to exacting safety standards in the rapidly evolving field of electromagnetic technology. With its promising performance and potential for widespread adoption, the AVPC can contribute to the sustainable development of transportation and other sectors.

Author Contributions: Article outline and conceptualization, S.L.; methodology, experiment, and writing—original draft preparation, Z.S. and J.X.; investigation and writing—review and editing, T.L.; project administration and funding acquisition, S.L., Y.Z. and X.Y. All authors have read and agreed to the published version of the manuscript.

Funding: This work was supported in part by the National Natural Science Foundation of China under Grant: (No. 52067011) and in part by Yunnan Fundamental Research Project under Grant (No. 202301AT070429) and also supported by Yunnan Province Major Science and Technology Project (Project No.: 202402AF080001).

Data Availability Statement: Dataset available on reqeust from the authors.

Conflicts of Interest: Authors Xi Yang and Yu Zhao were employed by the company Yunnan Energy Research Institute Co., Ltd. The remaining authors declare that the research was conducted in the absence of any commercial or financial relationships that could be construed as a potential conflict of interest.

References

1. Jawad, A.M.; Nordin, R.; Gharghan, S.K.; Jawad, H.M.; Ismail, M. Opportunities and Challenges for Near-Field Wireless Power Transfer: A Review. *Energies* **2017**, *10*, 1022. [CrossRef]
2. Barman, S.D.; Reza, A.W.; Kumar, N.; Karim, M.E.; Munir, A.B. Wireless Powering by Magnetic Resonant Coupling: Recent Trends in Wireless Power Transfer System and Its Applications. *Renew. Sustain. Energy Rev.* **2015**, *51*, 1525–1552. [CrossRef]
3. Hui, S.Y.R.; Zhong, W.; Lee, C.K. A Critical Review of Recent Progress in Mid-Range Wireless Power Transfer. *IEEE Trans. Power Electron.* **2014**, *29*, 4500–4511. [CrossRef]
4. Covic, G.A.; Boys, J.T. Modern Trends in Inductive Power Transfer for Transportation Applications. *IEEE J. Emerg. Sel. Top. Power Electron.* **2013**, *1*, 28–41. [CrossRef]
5. Chopra, S.; Bauer, P. Driving Range Extension of EV With On-Road Contactless Power Transfer—A Case Study. *IEEE Trans. Ind. Electron.* **2013**, *60*, 329–338. [CrossRef]
6. Xia, J.; Yuan, X.; Lu, S.; Dai, W.; Li, T.; Li, J.; Li, S. A General Parameter Optimization Method for a Capacitive Power Transfer System with an Asymmetrical Structure. *Electronics* **2022**, *11*, 922. [CrossRef]
7. Dai, J.; Ludois, D.C. A Survey of Wireless Power Transfer and a Critical Comparison of Inductive and Capacitive Coupling for Small Gap Applications. *IEEE Trans. Power Electron.* **2015**, *30*, 6017–6029. [CrossRef]
8. Kim, J.; Kim, D.-H.; Park, Y.-J. Analysis of Capacitive Impedance Matching Networks for Simultaneous Wireless Power Transfer to Multiple Devices. *IEEE Trans. Ind. Electron.* **2015**, *62*, 2807–2813. [CrossRef]
9. Li, T.; Li, S.; Liu, Z.; Fang, Y.; Xiao, Z.; Shafiq, Z.; Lu, S. Enhancing V2G Applications: Analysis and Optimization of a CC/CV Bidirectional IPT System with Wide Range ZVS. *IEEE Trans. Transp. Electrific.* **2024**, 1. [CrossRef]
10. Cruciani, S.; Campi, T.; Maradei, F.; Feliziani, M. Wireless Charging in Electric Vehicles: EMI/EMC Risk Mitigation in Pacemakers by Active Coils. In Proceedings of the 2019 IEEE PELS Workshop on Emerging Technologies: Wireless Power Transfer (WoW), London, UK, 18–21 June 2019; IEEE: London, UK, 2019; pp. 173–176.
11. Lu, X.; Wang, P.; Niyato, D.; Kim, D.I.; Han, Z. Wireless Charging Technologies: Fundamentals, Standards, and Network Applications. *IEEE Commun. Surv. Tutor.* **2016**, *18*, 1413–1452. [CrossRef]
12. Kalwar, K.A.; Aamir, M.; Mekhilef, S. Inductively Coupled Power Transfer (ICPT) for Electric Vehicle Charging—A Review. *Renew. Sustain. Energy Rev.* **2015**, *47*, 462–475. [CrossRef]
13. Li, S.; Yu, X.; Yuan, Y.; Lu, S.; Li, T. A Novel High-Voltage Power Supply With MHz WPT Techniques: Achieving High-Efficiency, High-Isolation, and High-Power-Density. *IEEE Trans. Power Electron.* **2023**, *38*, 14794–14805. [CrossRef]
14. Yashima, Y.; Omori, H.; Morizane, T.; Kimura, N.; Nakaoka, M. Leakage Magnetic Field Reduction from Wireless Power Transfer System Embedding New Eddy Current-Based Shielding Method. In Proceedings of the 2015 International Conference on Electrical Drives and Power Electronics (EDPE), Tatranska Lomnica, Slovakia, 21–23 September 2015; IEEE: Tatranska Lomnica, Slovakia, 2015; pp. 241–245.
15. Deng, J.; Li, W.; Nguyen, T.D.; Li, S.; Mi, C.C. Compact and Efficient Bipolar Coupler for Wireless Power Chargers: Design and Analysis. *IEEE Trans. Power Electron.* **2015**, *30*, 6130–6140. [CrossRef]

16. Mei, Y.; Wu, J.; He, X. Common Mode Noise Analysis for Inductive Power Transfer System Based on Distributed Stray Capacitance Model. *IEEE Trans. Power Electron.* **2022**, *37*, 1132–1145. [CrossRef]
17. Estrada, J.; Sinha, S.; Regensburger, B.; Afridi, K.; Popovic, Z. Capacitive Wireless Powering for Electric Vehicles with Near-Field Phased Arrays. In Proceedings of the 2017 47th European Microwave Conference (EuMC), Nuremberg, Germany, 10–12 October 2017; IEEE: Nuremberg, Germany, 2017; pp. 196–199.
18. Mai, J.; Wang, Y.; Zeng, X.; Yao, Y.; Wu, K.; Xu, D. A Multi-Segment Compensation Method for Improving Power Density of Long-Distance IPT System. *IEEE Trans. Ind. Electron.* **2022**, *69*, 12795–12806. [CrossRef]
19. Shafiq, Z.; Xia, J.; Min, Q.; Li, S.; Lu, S. Study of the Induced Electric Field Effect on Inductive Power Transfer System. In Proceedings of the 2021 IEEE PELS Workshop on Emerging Technologies: Wireless Power Transfer (WoW), San Diego, CA, USA, 1–4 June 2021; IEEE: San Diego, CA, USA, 2021; pp. 1–5.
20. Kim, M.; Ahn, S.; Kim, H. Magnetic Design of a Three-Phase Wireless Power Transfer System for EMF Reduction. In Proceedings of the 2014 IEEE Wireless Power Transfer Conference, Jeju City, South Korea, 8–9 May 2014; IEEE: Jeju City, South Korea, 2014; pp. 17–20.
21. Liu, Z.; Li, T.; Li, S.; Mi, C.C. Advancements and Challenges in Wireless Power Transfer: A Comprehensive Review. *Nexus* **2024**, *1*, 100014. [CrossRef]
22. Choi, S.Y.; Gu, B.W.; Jeong, S.Y.; Rim, C.T. Advances in Wireless Power Transfer Systems for Roadway-Powered Electric Vehicles. *IEEE J. Emerg. Sel. Top. Power Electron.* **2015**, *3*, 18–36. [CrossRef]
23. Budhia, M.; Covic, G.A.; Boys, J.T. Design and Optimization of Circular Magnetic Structures for Lumped Inductive Power Transfer Systems. *IEEE Trans. Power Electron.* **2011**, *26*, 3096–3108. [CrossRef]
24. Kim, J.; Kim, J.; Kong, S.; Kim, H.; Suh, I.-S.; Suh, N.P.; Cho, D.-H.; Kim, J.; Ahn, S. Coil Design and Shielding Methods for a Magnetic Resonant Wireless Power Transfer System. *Proc. IEEE* **2013**, *101*, 1332–1342. [CrossRef]
25. Siqi, L.; Mi, C. Wireless Power Transfer for Electric Vehicle Applications. *IEEE J. Emerg. Sel. Top. Power Electron.* **2015**, *3*, 4–17. [CrossRef]
26. Campi, T.; Cruciani, S.; Maradei, F.; Feliziani, M. Near-Field Reduction in a Wireless Power Transfer System Using LCC Compensation. *IEEE Trans. Electromagn. Compat.* **2017**, *59*, 686–694. [CrossRef]
27. Stepins, D.; Zakis, J.; Padmanaban, P.; Deveshkumar Shah, D. Suppression of Radiated Emissions from Inductive-Resonant Wireless Power Transfer Systems by Using Spread-Spectrum Technique. *Electronics* **2022**, *11*, 730. [CrossRef]
28. Inoue, K.; Kusaka, K.; Itoh, J.-I. Reduction in Radiation Noise Level for Inductive Power Transfer Systems Using Spread Spectrum Techniques. *IEEE Trans. Power Electron.* **2018**, *33*, 3076–3085. [CrossRef]
29. Park, S. Evaluation of Electromagnetic Exposure During 85 kHz Wireless Power Transfer for Electric Vehicles. *IEEE Trans. Magn.* **2018**, *54*, 5100208. [CrossRef]
30. Duan, X.; Lan, J.; Kodera, S.; Kirchner, J.; Fischer, G.; Hirata, A. Wireless Power Transfer Systems With Composite Cores for Magnetic Field Shielding With Electric Vehicles. *IEEE Access* **2023**, *11*, 144887–144901. [CrossRef]
31. Li, T.; Yuan, Y.; Xiao, Z.; Fang, Y.; Xingpeng, Y.; Li, S. Large Space Wireless Power Transfer System That Meets Human Electromagnetic Safety Limits. In Proceedings of the 2023 IEEE Wireless Power Technology Conference and Expo (WPTCE), San Diego, CA, USA, 4–8 June 2023; IEEE: San Diego, CA, USA, 2023; pp. 1–6.
32. *Guidelines on Limiting Exposure to Non-Ionizing Radiation: A Reference Book Based on the Guidelines on Limiting Exposure to Non-Ionizing Radiation and Statements on Special Applications*; Matthes, R.; Bernhardt, J.H. (Eds.) ICNIRP; International Commission on Non-Ionizing Radiation Protection: Oberschleißheim, Germany, 1999; ISBN 978-3-9804789-6-0.
33. International Commission on Non-Ionizing Radiation Protection. Guidelines for limiting exposure to time-varying electric and magnetic fields (1 Hz to 100 kHz). *Health Phys.* **2010**, *99*, 818–836. [CrossRef]
34. Jo, M.; Sato, Y.; Kaneko, Y.; Abe, S. Methods for Reducing Leakage Electric Field of a Wireless Power Transfer System for Electric Vehicles. In Proceedings of the 2014 IEEE Energy Conversion Congress and Exposition (ECCE), Pittsburgh, PA, USA, 14–18 September 2014; IEEE: Pittsburgh, PA, USA, 2014; pp. 1762–1769.
35. Wang, B.; Yerazunis, W.; Teo, K.H. Wireless Power Transfer: Metamaterials and Array of Coupled Resonators. *Proc. IEEE* **2013**, *101*, 1359–1368. [CrossRef]
36. Sample, A.; Smith, J.R. Experimental Results with Two Wireless Power Transfer Systems. In Proceedings of the 2009 IEEE Radio and Wireless Symposium, San Diego, CA, USA, 18–22 January 2009; IEEE: San Diego, CA, USA, 2009; pp. 16–18.
37. Sample, A.P.; Meyer, D.A.; Smith, J.R. Analysis, Experimental Results, and Range Adaptation of Magnetically Coupled Resonators for Wireless Power Transfer. *IEEE Trans. Ind. Electron.* **2011**, *58*, 544–554. [CrossRef]
38. Shahjalal, M.; Shams, T.; Tasnim, M.N.; Ahmed, M.R.; Ahsan, M.; Haider, J. A Critical Review on Charging Technologies of Electric Vehicles. *Energies* **2022**, *15*, 8239. [CrossRef]
39. Hayt, W. Engineering Electromagnetics. In *Physical Constants*; McGraw-Hill Companies: New York, NY, USA, 1974.
40. Paul, C.R. *Introduction to Electromagnetic Compatibility*; John Wiley & Sons: Hoboken, NJ, USA, 2022.
41. Tumanski, S. Induction Coil Sensors—A Review. *Meas. Sci. Technol.* **2007**, *18*, R31–R46. [CrossRef]

42. Kurokawa, K. Power Waves and the Scattering Matrix. *IEEE Trans. Microw. Theory Techn.* **1965**, *13*, 194–202. [CrossRef]
43. Sirbu, I.-G.; Mandache, L. Comparative Analysis of Different Topologies for Wireless Power Transfer Systems. In Proceedings of the 2017 IEEE International Conference on Environment and Electrical Engineering and 2017 IEEE Industrial and Commercial Power Systems Europe (EEEIC/I&CPS Europe), Milan, Italy, 6–9 June 2017; IEEE: Milan, Italy, 2017; pp. 1–6.